JOURNAL OF CATALYSIS 27, 266–274 (1972)

ESR Study of the Chromium Oxide—Potassium Oxide System

A. ANDREEV, N. NESHEV, D. MIHAJLOVA, L. PRAHOV, AND D. SHOPOV

Institute of Organic Chemistry, Bulgarian Academy of Sciences, Sofia 13, Bulgaria

Received February 24, 1972

An ESR investigation of chromium oxide samples containing potassium oxide has been carried out. It is shown that two kinds of defect structures can be considered in connection with the Cr^{3+} vacancy and K^+ and Cr^{6+} ions in the α-Cr_2O_3 lattice. The observed fine structure is interpreted with the aid of axially symmetric spin Hamiltonian parameters $g = 1.98$, $D_1 = 0.28$ cm^{-1}; and $g = 1.98$, $D_2 = 0.33$ cm^{-1}. The defect structures and their changes in the working conditions of the catalyst are linked with the activation and regeneration of chromium catalysts for dehydrogenation and dehydrocyclization of hydrocarbons.

Chromium catalysts usually contain potassium oxide as a promotor. The investigations (*1–5*) on the influence of alkaline additives on the catalytic activity of chromium catalysts do not fully clarify this question. The participation of Cr^{6+} ions in the formation of the active surface of the catalysts (*5, 6*) and their influence in the regeneration and activation by hydrogen (*6–8*) also pose additional questions to be answered.

The present investigation aims at studying the interaction between chromium and potassium oxides with the view to elucidating the promotor effect of potassium in chromium catalysts. Combined studies by different methods were carried with the purpose of obtaining information about the environment of chromium ions in the chromium oxide lattice when the potassium is added.

Experimental Methods

The samples were prepared by two different methods: (a) a wet mixture of CrO_3 and KCl in appropriate ratios was dried and then calcined in air at 800°C; and (b) chromium hydroxide precipitated from chromium nitrate by ammonia was dried at 100°C, KOH was added, and the dried mixture was calcined in air at 800°C. Analytical grade reagents were used. All samples studied are characterized in Table 1.

The amount of surface Cr^{6+} ions as CrO_4^{2-} was obtained by water extraction and titration. The total Cr^{6+} concentration was determined by the Bunsen–Rupp method as described in (*9*). The surface area of the samples was determined by low temperature adsorption of air.

The hydrogen used was purified by a "deoxo" unit and then passed through a liquid-nitrogen trap. In some cases the treatment of the samples was carried out in a standard high-vacuum system permitting evacuation down to 1×10^{-5} Torr and equipped with a gas dosage system.

The spectra were recorded on a JEOL-3BS spectrometer at an X-band frequency and a manganese standard was employed for the determination of the g-value and linewidth. A Faraday balance was used to determine the magnetic susceptibility at 25°C. Optical spectra were obtained with a VSU-2P "Zeiss-Jena" spectrophotometer and reflectance attachment using MgO as a reference in the 250–650 nm wavelength region.

TABLE 1

Designation	Chemical composition (weight percent)		Mode of preparation	Calcination time (hr)	Surface Cr^{6+} concentration[a] (mg/g sample)	Cr^{6+} total concentration obtained by dissolution in HCl (mg/g sample)	Surface area (m^2/g)	Magnetic susceptibility ($\mathcal{K} \times 10^{-6}$)
	Cr_2O_3	K_2O						
1	100.0	—	from CrO_3	2	0.16	0.2	2.3	23.0
2	98.0	2.0	from CrO_3 and KCl	2	13.60	21.5	1.0	24.4
3	99.5	0.5	from CrO_3 and KCl	4	2.80	3.3	2.0	24.5
4	98.0	2.0	from CrO_3 and KCl	4	15.00	16.0	0.8	23.2
5	95.0	5.0	from CrO_3 and KCl	4	32.60	36.7	0.2	21.1
6	100.0	—	from chromium hydroxide	2	0.72	—	13.4	—
7	99.6	0.4	from chromium hydroxide and KOH	6	2.58	—	13.5	—
8	98.0	2.0	sample 4 after water extraction	—	—	0.4	1.3	—

[a] Obtained by water extraction.

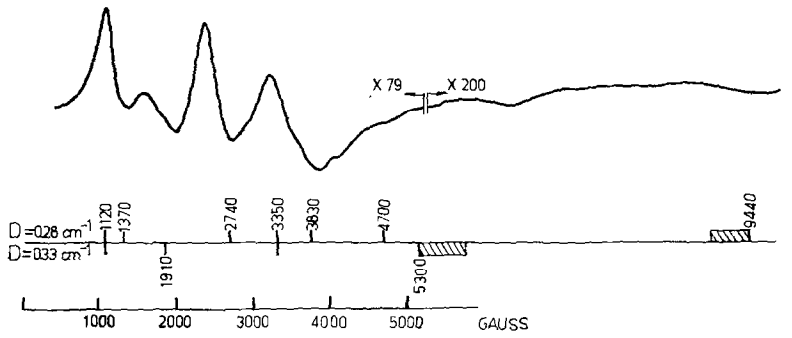

FIG. 1. ESR spectrum of sample 4 at room temperature.

RESULTS

Sample 1 (without potassium) did not give rise to an ESR signal. The ESR spectrum of sample 4, containing 2% K_2O, is shown in Fig. 1. A fine structure is observed in the spectra recorded at room temperature.

Figure 2 depicts the ESR spectrum of sample 7, which has the same fine structure, but exhibits a small difference between the intensities of the different lines of the fine structure. At $g = 2.03$ a narrow line appears with a linewidth of 50 G.

The characteristic ESR signal is not observed if the sample is prepared in vacuum.

On Fig. 3 are shown ESR spectra of equal weight of samples 3–5 recorded under identical conditions and amplifications, which permits the evaluation of the relative intensities of the ESR signals. All three samples exhibit identical positions of the fine-structure lines, the sole difference between them being the amplitudes.

The spectrum of sample 4 after evacuation down to 10^{-5} Torr for 2 hr at 800°C is presented in Fig. 4.

It was established that the intensity of the ESR signal of sample 4 did not change after extraction with water which resulted in a considerable amount of Cr^{6+} ions leaving the sample (Table 1).

The three transitions $({}^4A_{2g} \rightarrow {}^4T_2), T_f$ $({}^4A_{2g} \rightarrow {}^4T_{2g})$, and $T_p({}^4A_{2g} \rightarrow {}^4T_{1g}({}^4P))$, associated with octahedral Cr^{3+} were observable in the optical reflectance spectra (*10–12*). The third transition is not well-defined since it occurs as a shoulder on the charge-transfer band. The Δ value can be evaluated from the first band position and the value B_{35} from the second. According to the MO treatment this value is proportional to the e_g and t_{2g} orbital Coulomb integral (*12*). The values of Δ and B_{35} for all samples studied are given in Table 2.

Magnetic susceptibility determination results at room temperature are listed in Table 1.

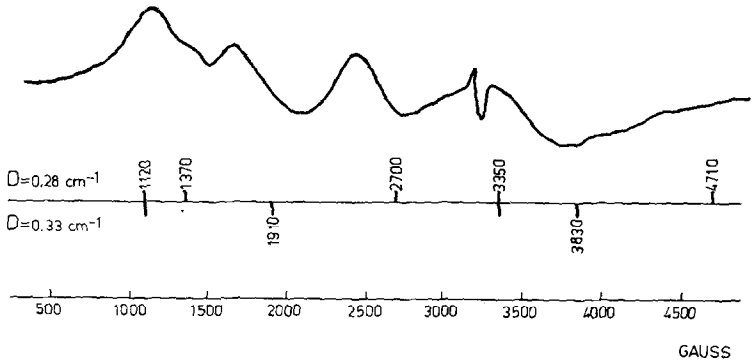

FIG. 2. ESR spectrum of sample 7 at room temperature.

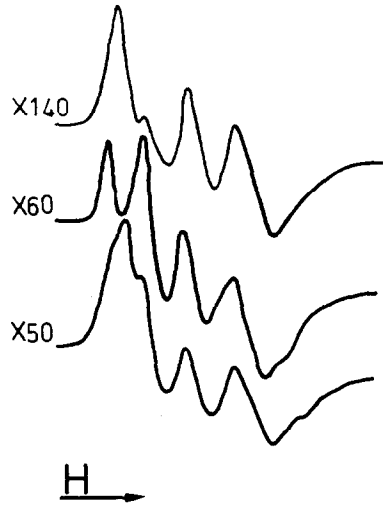

FIG. 3. ESR spectra of equal weights of samples 3–5 at room temperature.

The results from ESR investigation of pure chromium oxide can be summarized as follows. Sample 1 prepared from CrO_3 did not show an ESR signal. Sample 6 prepared from hydroxide with bigger surface area, gives a broad (1000 G) signal at $g = 1.98$ remains. Reduction with n-heptane cooling to room temperature in hydrogen the signal disappeared. No ESR signal could be observed if the hydroxide decomposition, high temperature treatment at 800°C, and cooling to room temperature was carried out under vacuum.

Figure 5 shows the ESR spectra of sample 4 (containing 2% K_2O) after reduction at 550°C and hydrogen pressure of 200 Torr and the spectra of the same sample after reduction with hydrogen at 750°C at

TABLE 2
OPTICAL REFLECTANCE SPECTRA PARAMETERS

Sample	$\Delta(cm^{-1})$	$B_{35}(cm^{-1})$
1	16660	480
2	16660	480
3	16600	460
4	16660	480
5	16670	500
6	16600	470
8	16660	480
1[a]	16600	460

[a] Reduced in hydrogen 2 hr at 800°C.

the same hydrogen pressure. A strong signal at $g = 1.98$ and a linewidth of 320 G is superimposed upon the fine-structure signals when the reduction is carried out at 550°C. Reduction with hydrogen at 750°C leads to a complete disappearance of the fine structure and only the signal at $g = 1.98$ remains. Reduction with n-heptane at 25 Torr results in the appearance of the same signal at $g = 1.98$ but with a linewidth of 260 G.

On Fig. 6 is represented the spectrum of sample 4 oxidized in air at 550°C for 2 hr after reduction in hydrogen at 750°C. The intensity of the signal at $g = 1.98$ diminished and no well-resolved fine structure appears. A well-defined fine structure is produced and the signal at $g = 1.98$ is completely destroyed if the oxidation is carried out at 750°C.

When consecutive cycles of reduction by hydrogen at 450°C and oxidation at 750°C of sample 7 containing 0.4% K_2O were carried out the linewidth of the signal at

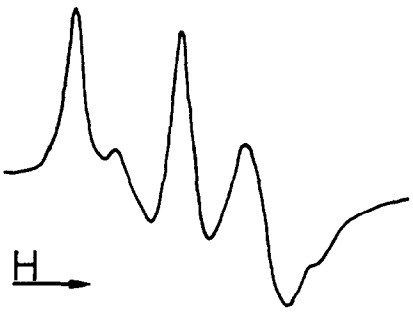

FIG. 4. ESR spectrum of sample 4 after evacuation for 2 hr at 800°C.

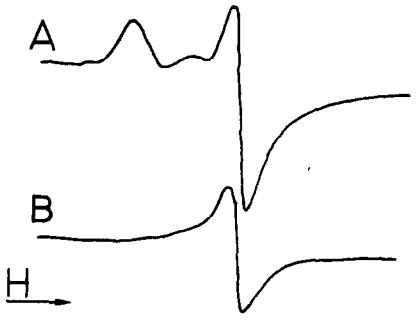

FIG. 5. ESR spectra of sample 4 after reduction with hydrogen at 550°C (A), and at 750°C (B).

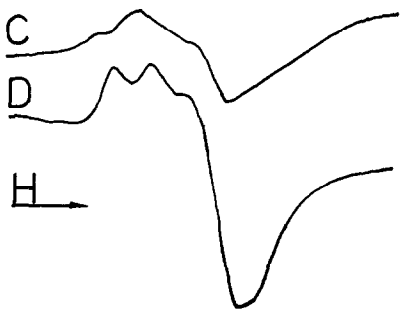

FIG. 6. ESR spectra of sample 4 oxidized at 550°C (C), and 750°C (D) after reduction with hydrogen at 750°C.

$g = 1.98$ for the first cycle was 230 G; the linewidth did not change further after several more cycles.

DISCUSSION

The results show that the presence of potassium in the samples causes the appearance of the fine structure in the ESR spectrum. Slinkin and Fedorovskaja (*13*) observed a fine structure in the ESR spectra of Cr_2O_3 containing Li^+ ions and assumed that the spectrum observed is due to the Cr^{3+} ions in the chromium alum-like crystal field. Addition of lithium to magnesium oxide containing Cr^{3+} ions results in the formation of defect structures corresponding to Cr^{3+} ions at sites in the neighbourhood of the Mg^{2+} valances with tetragonal symmetry and appropriate D values (*14*, *15*).

The fine structure in the ESR spectrum of such magnetoconcentrated system as the chromium oxide one can be explained with the diminished exchange-coupling between some of the Cr^{3+} ions and axial distortion of the crystal field. It was assumed for some Cr_2O_3-containing systems (*11*, *16*), that most probably magnetic diluents are the Cr^{6+} ions. As the results of the chemical analysis shown in Table 1 indicate, that the presence of potassium in the samples increases the amount of Cr^{6+} ions. When the concentration of potassium in the samples increases and the time of calcination is prolonged, part of the Cr^{3+} ions is transformed into the chromate phase and a small decrease in magnetic susceptibility together with a change in ESR signal takes place as well. The increase in B_{35} value when potassium is added (Table 2) also supports the concept of spin decoupling to some extent in the α-Cr_2O_3, caused by the decrease in Cr^{3+}–Cr^{3+} interaction increases the repulsion integral B_{35} (*12*).

Spin decoupling caused by Cr^{6+} ions embedded mainly on the surface layers of the pure chromium oxide may be also the reason for the appearance of the ESR signal for the sample 6 (pure chromium oxide with larger surface area). Chromium oxide studies with infrared spectroscopy showed the presence of $(Cr{=}O)^{4+}$ groups on the surface (*17*). Many other results (*9*) have confirmed the existence of surface oxidation of Cr_2O_3.

Substitution of some Cr^{3+} ions and an increase of astoichiometric oxygen in the Cr_2O_3 lattice creates the cation vacancies and the associated Cr^{3+} ions in sites with axially distorted crystal fields (*14*). If the symmetry around the Cr^{3+} ions is lowered from cubic to tetragonal by some local perturbation, the electron spin resonance spectrum will be described by an axially symmetric spin Hamiltonian of the form:

$$\mathcal{H} = g\beta H_z \hat{S}_z + D\left(\hat{S}_z^2 - \frac{5}{4}\right), \qquad (1)$$

where z refers to the axis of distortion.

The possibilities of the interpretation the ESR spectrum of Cr^{3+} in powdered systems have been extensively discussed by van Reijen (*18*). If Θ is the angle between the symmetry axis in the crystal (for the present case the axis of distortion) and the direction of the field, the dependence of the resonance field on Θ could be computed for every one of the six possible transitions for different values of D. The polycrystalline species will exhibit resonance absorption at values of the magnetic field H for which $\partial H/\partial \cos\Theta$ is small. It is possible to evaluate approximately the D term for a polycrystalline sample by comparing the experimental spectra with the calculated H_{res}/Θ dependences for different D. It was found in this way that the experimental spectra depicted in Figs. 1 and 2 could be satisfactorily interpreted by employing two

different values of D. The following spin-Hamiltonian parameters were found, $D = 0.28$ cm^{-1}, $g = 1.98$, and $D = 0.33$ cm^{-1}, $g = 1.98$. In Fig. 7, the H_{res}/Θ dependence for $D = 0.28$ cm^{-1} and $g = 1.98$ for every $M_s \rightarrow M'_s$ transition is given. Two close values for D in the Cr^{3+} ESR spectrum in tetragonal field were reported by other authors as well (*14*).

Some possibilities concerning the structure of centers with axially distorted fields around the Cr^{3+} ions can be discussed. In Fig. 8 is represented part of the projection of the corundum structure on the (210) plane (*11*). If we consider the ionic radii of Cr^{3+}—0.55 Å, Cr^{6+}—0.52 Å and K^+—1.33 Å (*19*), it is natural to suppose that Cr^{6+} can replace the Cr^{3+} ion sites in α–Cr_2O_3 lattice, but K^+ will most probably be situated in the octahedral holes as

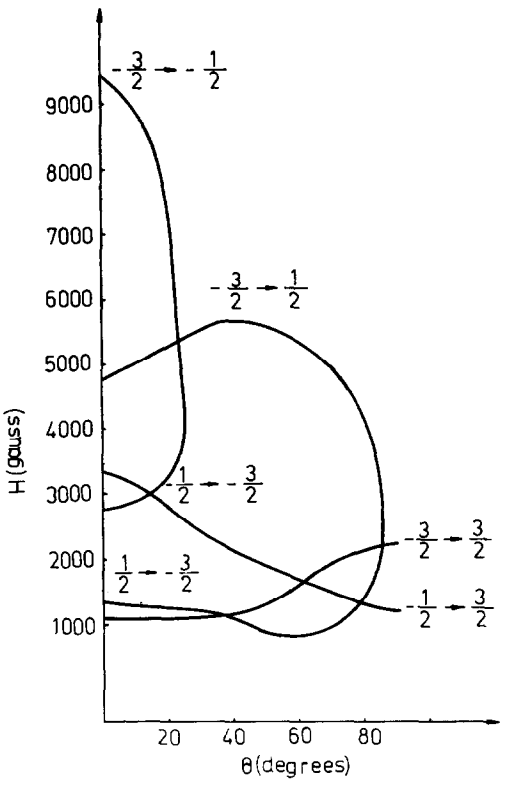

FIG. 7. Theoretically calculated positions of the resonance signal as a function of the orientation of the magnetic field for $D = 0.28$ cm^{-1} and $g = 1.98$. The curves are labeled by their $M_s \rightarrow M'_s$ transitions.

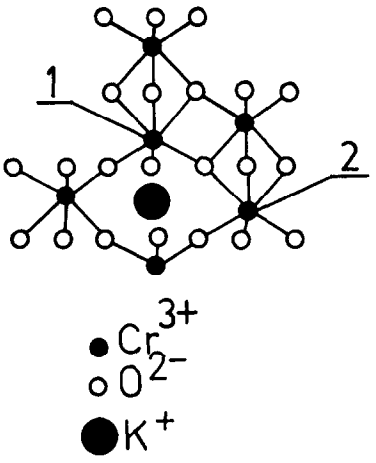

FIG. 8. Projection of the corundum structure on the (210) plane is shown; 1 and 2—positions of the Cr^{3+} vacancy.

shown in Fig. 8. The position of the cation Cr^{3+} vacancies are shown as 1 and 2, respectively, for $D = 0.28$ cm^{-1}, and for $D = 0.33$ cm^{-1} according to the electroneutrality principal for a crystal lattice. Some theoretical speculations could be useful for confirmation of the possibility of existence of the proposed defect structures. The exact structure of the defects, shown in Fig. 8 as 1 and 2, was constructed taking into account the Cr^{6+} ions for the preservation of lattice electroneutrality. The crystal field symmetry around the Cr^{3+} next to the vacancy 1 or 2 is distorted, thus leading to the change of the trigonality parameter V (*20*). The spin-Hamiltonian (*1*) parameter D is given (*21*) by the equation:

$$D = k(v/\Delta^2), \qquad (2)$$

where k is a constant. The v and Δ values can be evaluated if the potential is created from a Cr^{3+} vacancy. Cr^{6+} and K^+ are presented in spherical functions and the quantum axis with C_3 symmetry is used (*22*). The calculations showed that the difference between Δ_1 and Δ_2 is too small for consideration and therefore $D_2/D_1 = v_2/v_1 = 1.21$. The value of D_2/D_1 is very close to the experimental one of 1.18. The theoretical D_2/D_1 ratio is in support of the proposed defect structures.

Resonance adsorption at 1910 G ($\Theta = 0$) is characteristic for $D = 0.33$ cm^{-1} (defect

type 2). The relative intensity of this resonance line is the measure for the concentration of type 2 defects depending on alkali concentration (Fig. 3) and thermal treatment. When the sample is treated in vacuum at 800°C it loses some of its astoichiometric oxygen and more of the defects of the type 2 disappear because of their lower stability. It was established that the treatment of sample 4 at 800°C under vacuum leads to a relative decrease of the signal at 1900 G (Fig. 4).

The magnetic susceptibility measurements gave evidence in support of local defect formation but not of a new phase containing Cr^{3+} ions entirely free from the exchange interaction. Otherwise, there should be considerable increase in the magnetic susceptibility.

The rise in the Cr^{6+} ions and defect concentration to very high values resulted in the borderline case in the formation of a new chromate phase, and the fine structure disappeared. In the reflectance spectra of sample 5 with high potassium concentration, absorption at 25600 cm^{-1} and a shoulder at 39200 cm^{-1} appear, because of charge transfer bands of CrO_4^{2-} ions (*23*).

The introduction of Cr^{3+} in the chromate phase may be regarded as responsible for the fine structure in the ESR spectrum too. The partial reduction of K_2CrO_4 and $K_2Cr_2O_7$ with hydrogen creates favorable conditions for the formation of Cr^{3+} ions and their introduction into the chromate crystal. In this case no fine structure in the ESR spectra is observed, which refutes the above-mentioned possibility. This was confirmed conclusively when the extraction with water of the chromate phase of the sample was carried out and no change in the intensity of the fine structure was observed after its removal.

Attention must be given to the asymmetric resonance line in the spectrum of sample 7 (prepared by more prolonged temperature treatment) at $g = 2.03$ at linewidth of 50 G. A possible explanation for this line is the presence of Cr^{5+} ions in the square pyramidal surroundings on the surface. The g value observed is quite high but g higher than 2.0023 are in the some cases characteristic for d^1 configuration, for example, $CrOCl_5^{2+}$ (*24*) and $CrOBr_5^{2-}$ (*25*).

Changes in the fine structure during different treatments resembling the activation and regeneration cycle of the chromium catalyst for dehydrogenation and dehydrocyclization of paraffin hydrocarbons provide a possibility for some explanations connected with the promotor action of potassium. It can be suggested from general considerations that defect structures in the crystal lattice may take part in the catalytic reactions (*26*). It was firmly established that the presence of some amounts of Cr^{6+} is necessary in order to the catalyst to be sufficiently active for *n*-butane dehydrogenation and *n*-heptane dehydrocyclization (*1*). At the above-mentioned reaction conditions (550°C) the fine structure cannot be removed by hydrogen and hydrocarbon treatment (Fig. 5), which is an indication of the stability of the defects in the catalyst under these conditions. When sample 4 was reduced at 750°C the fine structure in the ESR spectrum disappeared (Fig. 5). At the same time preliminary treatment with hydrogen at 750°C of the dehydrocyclization catalyst decreased the latter's activity (*7*), but had no effect on the catalyst not containing alkali promotor.

Regeneration with air restored *n*-butane dehydrogenation (*3*) and *n*-hexane dehydrocyclization (*7*) catalytic activity, and was carried out at 700°C. Temperature treatment in air at 550°C is not sufficient for restoring initial activity. It is clear from the results shown in Fig. 6 that the fine structure is not restored by calcination of the reduced catalyst at 550°C in air, but calcination at 750°C is necessary.

As already mentioned (Fig. 4), a vacuum treatment of sample 4 leads to the disappearance of some of the defect structures because of the decrease of astoichiometric oxygen. An analogous effect must be expected for the high-temperature treatment in an inert gas. The decrease of yields in the dehydrocyclization of *n*-heptane (*27*) over the chromium–aluminium–potassium catalyst was established when the catalyst

had been treated at high temperature in helium. The defect structures in the potassium-dotted chromium oxide evaluated by ESR spectra play an important in catalytic activity as it becomes clear from the above discussed experimental results.

The chromate phase is not directly responsible for catalytic activity. Potassium addition above an optimum percentage does not increase the activity of the chromium–aluminium catalyst (*8*, *28*) in spite of the fact that the chromate phase increases (*29*). The present results show (Fig. 3) that the intensity of the fine structure goes through a maximum, but simultaneously the Cr^{6+} ion concentration increases continuously with potassium concentration.

Another possibility for potassium promotor action arises. When the potassium-containing samples were reduced with hydrogen or a hydrocarbon, a strong ESR signal at $g = 1.98$ with a linewidth of 320 G appeared. This is an antiferromagnetic resonance from the fine crystal particles of α-Cr_2O_3 obtained from the reduction of a Cr^{6+}-containing phase, possibly with high catalytic activity.

The first of the two possibilities discussed, that is, defect structure formation, is more likely, one, because it is much more consistent with the experimental data. It is possible that the structures of the defect may be connected in some way with the low valence chromium ions Cr^{2+} and Cr^{4+} (*30*, *31*) and the decrease of the effect of exchange interaction should also be considered (*32*, *33*).

The present investigation of the Cr_2O_3–K_2O showed the presence of the defect structures connected with the introduction of K^+ and Cr^{6+} ions into the Cr_2O_3 lattice which is very likely to play an important role in the catalytic activity of chromium catalysts.

References

1. Rozengart, M. I., and Kazanskii, B. A. *Usp. Khim.* **40**, 1537 (1971).
2. Carra, S., Forni, L., and Vitani, C., *J. Catal.* **9**, 154 (1967).
3. Rubinshchein, A. M., Pribitkova, N. A., Afanasiev, V. A., and Slinkin, A. A., *Kinet. Katal.* **1**, 129 (1960).
4. Isagulyants, G. V., Slinkin, A. A., Gadzhikasumov, V. S., Fedorovskaja, E. A., and Gudkov, B. S., *Kinet. Katal.* **11**, 1184 (1970).
5. Poole, C. P., and McIver, D. S., *Advan. Catal.* **17**, 223 (1967).
6. Fridshtein, I. L., and Zimina, N. A., "Nauchnie Osnovi Podbora i Proizvodstva Katalizatorov," p. 274. Akad. Nauk. SSSR Sibirsk. Otdel., Novosibirsk, 1964.
7. Rosengart, M. I., Gitis, K. M., Saltanova, V. P., Anurov, C. A., Rachshupkina, Z. A., and Kazanskii, B. A., *Kinet. Katal.* **11**, 1446 (1970).
8. Fridshtein, I. L., and Zimina, N. A., "Nauchnie Osnovi Podbora i Proizvodstva Katalizatorov," p. 267. Akad. Nauk. SSSR Sibirsk. Otdel., Novosibirsk, 1964.
9. Deren, J., and Haber, J., *Ceramika* **13**, Krakov, 1969.
10. Poole, C. P., and Itzel, J. F., *J. Chem. Phys.* **39**, 3445 (1963).
11. Stone, F. S., and Vikermann, J. C., *Trans. Faraday Soc.* **67**, 316 (1971).
12. Reinen, D.. *Struct. Bonding (Berlin)* **6**, 30 (1969).
13. Slinkin, A. A., and Fedorovskaja, E. A., "Radiospectroskopija tverdogo tela," p. 283. Atomizdat, Moscow, 1967; *Dokl. Akad. Nauk. SSSR* **150**, 328 (1963).
14. Handerson, B., and Hall, T. P. P., *Proc. Phys. Soc.* **90**, 511 (1967).
15. Cordischi, D., Vikermann, J. C., and Cimino, A., *Trans. Faraday Soc.* **66**, 1312 (1970).
16. Ellison, A., Onbridge, J. O. V., and Sing, K. S. W., *Trans. Faraday Soc.* **66**, 1004 (1970).
17. Shopov, D. M., and Palazov, A. N., *Kinet. Katal.* **6**, 864 (1965).
18. van Reijen, L. L., Thesis, Eindhoven, 1964.
19. Pauling, L., "The Nature of the Chemical Bond," p. 514. Cornell University Press, New York, 1960.
20. Pryce, M. H., and Runciman, W. A., *Discuss. Faraday Soc.* **26**, 34 (1958).
21. Meijer, P. H., and Gerristen, H. J., *Phys. Rev.* **100**, 742 (1955).
22. Macfarlane, R. M., *J. Chem. Phys.* **39**, 3118 (1963).
23. Campbell, J. A., *Spectrochim. Acta* **21**, 1333 (1965).
24. Kon, H., and Sharpless, N. E., *J. Chem. Phys.* **42**, 906 (1965).
25. Kon, H., and Sharpless, N. E., *J. Phys. Chem.* **70**, 105 (1966).

26. DOWDEN, D. A., *J. Chem. Soc.* 242 (1950).
27. NOVIKOVA, L. A., ROZENGART, M. I., KONONOV, H. F., IVANOVA, N. G., ZUEVA, T. V., AND KAZANSKII, B. A., *Neftekhim.* **6,** 531 (1966).
28. KAZANSKII, B. A., DROGANSKII, A. Z., ROSENGART, M. I., BRECHSHENKO, E. M., REMIZOV, V. G., AND OGLOBINA, L. I., "Nauchnie Osnovi Podbora i Proizvodstva Katalizatorov," p. 312. Akad. Nauk. SSSR Sibirsk. Otdel., Novosibirsk, 1964.
29. POOLE, C. P., AND MCIVER, D. S., *Advan. Catal.* **17,** 223 (1967).
30. VAN REIJEN, L. L., SACHTLER, W. M. H., COSSEE, P., AND BROWER, D. M., *Proc. Int. Congr. Catal. 3rd 1964* **2,** 829 (1965).
31. PRZHEVALSKAJA, L. K., SHVETS, V. A., AND KAZANSKII, V. B., *Kinet. Katal.* **11,** 1310 (1970).
32. SHAPOVALOVA, U. A., BRYUHOVETSKAJA, I., AND VOEVODSKII, V. V., *Kinet. Katal.* **8,** 1314 (1967).
33. CIMINO, A., INDOVINA, V., PEPE, F., AND SCHIAVELO, M., 4th International Congress on Catalysis, Paper 12, Moscow, 1968.